University of Nebraska - Lincoln

DigitalCommons@University of Nebraska - Lincoln

Faculty Publications: Department of Entomology

Entomology, Department of

2018

Octapartite negative-sense RNA genome of High Plains wheat mosaic virus encodes two suppressors of RNA silencing

Adarsh K. Gupta
University of Nebraska -Lincoln, adarsh.bio@gmail.com

Gary L. Hein
University of Nebraska - Lincoln, ghein1@unl.edu

Robert A. Graybosch
USDA, Agricultural Research Service, bob.graybosch@ars.usda.gov

Satyanarayana Tatineni
USDA, Agricultural Research Service, Satyanarayana.Tatineni@ars.usda.gov
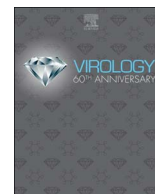
Follow this and additional works at: https://digitalcommons.unl.edu/entomologyfacpub

Part of the Entomology Commons

Octapartite negative-sense RNA genome of *High Plains wheat mosaic virus* encodes two suppressors of RNA silencing

Adarsh K. Gupta[a], Gary L. Hein[b], Robert A. Graybosch[c], Satyanarayana Tatineni[d],*

[a] Department of Plant Pathology, University of Nebraska-Lincoln, Lincoln, NE 68583, United States
[b] Department of Entomology, University of Nebraska-Lincoln, Lincoln, NE 68583, United States
[c] United States Department of Agriculture-Agricultural Research Service (USDA-ARS) and Department of Agronomy and Horticulture, University of Nebraska-Lincoln, Lincoln, NE 68583, United States
[d] USDA-ARS and Department of Plant Pathology, University of Nebraska-Lincoln, Lincoln, NE 68583, United States

ARTICLE INFO

ABSTRACT

High Plains wheat mosaic virus (HPWMoV, genus *Emaravirus*; family *Fimoviridae)*, transmitted by the wheat curl mite (*Aceria tosichella* Keifer), harbors a monocistronic octapartite single-stranded negative-sense RNA genome. In this study, putative proteins encoded by HPWMoV genomic RNAs 2–8 were screened for potential RNA silencing suppression activity by using a green fluorescent protein-based reporter agroinfiltration assay. We found that proteins encoded by RNAs 7 (P7) and 8 (P8) suppressed silencing induced by single- or double-stranded RNAs and efficiently suppressed the transitive pathway of RNA silencing. Additionally, a *Wheat streak mosaic virus* (WSMV, genus *Tritimovirus*; family *Potyviridae*) mutant lacking the suppressor of RNA silencing (ΔP1) but having either P7 or P8 from HPWMoV restored cell-to-cell and long-distance movement in wheat, thus indicating that P7 or P8 rescued silencing suppressor-deficient WSMV. Furthermore, HPWMoV P7 and P8 substantially enhanced the pathogenicity of *Potato virus X* in *Nicotiana benthamiana*. Collectively, these data demonstrate that the octapartite genome of HPWMoV encodes two suppressors of RNA silencing.

1. Introduction

RNA silencing or RNA interference is one of the most important and highly conserved gene regulation and host defense mechanisms in many eukaryotes (Fire et al., 1998; Li and Ding, 2006). Double-stranded RNAs (dsRNAs) derived from viral replicative intermediates (Cogoni and Macino, 2000), transposons (Aravin et al., 2001), or overexpressed transgenes (Wang and Metzlaff, 2005) are inducers of RNA silencing. These dsRNAs are diced into 21–24 nucleotide (nt) short-interfering RNAs (siRNAs) (Hamilton and Baulcombe, 1999; Ketting et al., 2001) by an RNase III type ribonuclease called Dicer (Dicer-like, DCL) (Bernstein et al., 2001; Fukudome et al., 2011). The siRNA duplexes are protected from exoribonucleases through 2′-O-methylation at their 3′ overhangs by a methyltransferase, HEN1 (Park et al., 2002). One of the strands of siRNA duplex is loaded onto Argonaute (AGO) proteins, the key players in the formation of RNA-induced silencing complex (RISC) effectors of siRNA that are involved in slicing of target RNAs based on sequence complementarity (Ding and Voinnet, 2007; Hammond et al., 2000; Holoch and Moazed, 2015). Thus, RNA silencing is an RNA-induced, sequence-specific, antiviral defense mechanism (Ding, 2010; Moazed, 2009).

Viruses have evolved by adopting several strategies to evade or counter the host RNA silencing-based defense machinery (Li and Ding, 2006). A few viruses escape silencing machinery by replicating within confined intracellular spherules (Schwartz et al., 2002) or by out-performing host dicing machinery through faster replication (Li and Ding, 2006). However, the most effective counterdefense response of viruses is mounted by encoding one or more suppressors of RNA silencing proteins (Csorba et al., 2015; Li and Ding, 2006). Suppressors of RNA silencing are highly divergent and interfere, inactivate, or degrade several key players of RNA silencing pathways involved in dsRNA binding (Mérai et al., 2006), dicing (Samuel et al., 2016), siRNA uptake (Silhavy et al., 2002), RISC assembly (Lu et al., 2005), and amplification (Fang et al., 2016).

The suppressors of RNA silencing of several positive-sense RNA viruses have been extensively studied, but only a few were reported from negative-sense RNA viruses. For example, the NSs and NS3 proteins encoded by ambisense RNA 3 in the plus-sense orientation of tospoviruses and tenuiviruses, respectively, have been reported as suppressors of RNA silencing (Bucher et al., 2003). In monopartite negative-sense RNA viruses, P6 of *Rice yellow stunt rhabdovirus* (Guo et al., 2013) and phosphoprotein of *Lettuce necrotic yellows*

---

cytorhabdovirus (Mann et al., 2015) also act as RNA silencing suppressors. Among human negative-sense RNA viruses, VP35 of *Ebola virus* (Haasnoot et al., 2007) and NS1 protein of *Human influenza virus* A are suppressors of RNA silencing (Li et al., 2004).

High Plains wheat mosaic virus (HPWMoV), previously named as High Plains virus, wheat mosaic virus, or maize red stripe virus, is an accepted species of the genus *Emaravirus* in the family *Fimoviridae* within the order *Bunyavirales* (ICTV, 2016; Tatineni et al., 2014a). Members of the genus *Emaravirus* are eriophyid mite-transmitted viruses with 4–8 single-stranded negative-sense genomic RNA segments, encoding a single open reading frame (ORF) in each genomic RNA segment (Mielke-Ehret and Mühlbach, 2012). HPWMoV is the causal agent of High Plains disease, an economically important disease of wheat (*Triticum aestivum* L.) and maize (*Zea mays* L.), and it is transmitted by eriophyid mite, wheat curl mite (*Aceria tosichella* Keifer) (Seifers et al., 1997; Skare et al., 2003). The virion particles of HPWMoV are roughly spherical glycoproteinaceous double membrane bodies with RNA segments encapsidated by nucleocapsid protein (Louie et al., 2006; Skare et al., 2006). The genome of HPWMoV is comprised of eight RNA segments in negative-sense orientation (Tatineni et al., 2014a). Proteins encoded by each of eight genomic RNA (RNA 1–8) segments were designated as P1 to P8, respectively. Through sequence identity, P1 is annotated as an RNA-dependent RNA polymerase, P2 as a glycoprotein with a potential post-translational cleavage site resulting in P2a and P2b, P3 as a nucleocapsid protein, and P4 as a movement protein. P5 and P6 possess weak amino acid homology with corresponding proteins of other emaraviruses with no known function. However, P7 and P8 show no significant sequence identity with any other proteins reported in GenBank (Tatineni et al., 2014a). Additionally, HPWMoV isolates from Nebraska and Kansas encode two variants of RNA 3 (3A and 3B) with 11% amino acid differences (Stewart, 2016; Tatineni et al., 2014a).

Functions of emaravirus-encoded proteins are poorly studied due to their recent genome characterization and non-availability of reverse genetics systems for their negative-sense RNA genomes. One exception is that P4, encoded by RNA 4 of *Fig mosaic virus* and *Raspberry leaf blotch virus* (RLBV), has been shown to be a movement protein (Ishikawa et al., 2013; Yu et al., 2013). There is no information on suppressors of RNA silencing proteins encoded by emaraviruses. In this study, we examined HPWMoV-encoded proteins to identify suppressors of RNA silencing by using a green fluorescent protein (GFP)-based agroinfiltration assay and demonstrate rescue of a silencing suppressor-deficient mutant of *Wheat streak mosaic virus* (WSMV) for systemic infection of wheat. We found that P7 and P8 proteins of the octapartite negative-sense RNA genome of HPWMoV suppress RNA silencing at the cellular level and the transitive pathway of RNA silencing. This is the first report that a multipartite negative-sense RNA virus in the family *Fimoviridae* encodes two suppressors of RNA silencing.

2. Results

2.1. Octapartite genome of HPWMoV encodes two suppressors of RNA silencing

The octapartite genome of HPWMoV encodes eight ORFs, one per genomic RNA segment, in viral complimentary orientation, flanked by untranslated regions of variable lengths (Fig. 1A; Tatineni et al., 2014a). To determine if any of the HPWMoV encoded proteins suppress RNA silencing in plant cells, we used the levels of GFP fluorescence expressed from a transient expression construct (35S-GFP; Qu et al., 2003) as the reporter for the silencing suppression activity of co-expressed HPWMoV proteins. The 35S-GFP construct, along with constructs designed to express various HPWMoV proteins, were delivered into *Nicotiana benthamiana* leaves via agroinfiltration. Specifically, HPWMoV ORFs encoding for P2a, P2b, P3, P4, P5, P6, P7 or P8 were placed downstream of the 35S promoter in the binary plasmid pCASS4

(a variant of pCASS2, Shi et al., 1997). *Triticum mosaic virus* (TriMV) P1 (pCASS-TriMV P1; Tatineni et al., 2012) and the empty pCASS4 vector were used as positive and negative controls, respectively. The infiltrated patches of *N. benthamiana* leaves showed bright GFP fluorescence under UV illumination at 2 days postinfiltration (dpi) in all the samples (data not shown). However, at 3 dpi, the intensity of green fluorescence was precipitously reduced in all the samples except with P7 and P8 (Fig. 1B). At 5 dpi, the green fluorescence remained with P7 and P8, albeit at lower levels compared to TriMV P1, but the fluorescence was completely lost with other HPWMoV ORFs (Fig. 1B). These data suggest that HPWMoV P7 and P8 possess suppressor of RNA silencing activity. The −1 frameshift mutants of P7 and P8 behaved similar to pCASS4 with no expression of GFP at 3 and 5 dpi, suggesting a role for protein but not for RNA sequence in suppression of RNA silencing activity (Fig. 1B).

The levels of silencing and silencing suppression of GFP were assayed by examining the accumulation of GFP-specific siRNAs and mRNA, respectively, in northern blot hybridizations using equal amounts of total RNA isolated at 3 and 5 dpi (Fig. 1C). GFP-specific mRNA accumulated in leaf patches infiltrated with P7 or P8, but siRNAs accumulated at significantly reduced levels (Fig. 1C). These data indicate that P7 and P8 interfere with sense transgene-induced silencing by affecting siRNA accumulation. The levels of fluorescence and GFP mRNA accumulation in P7 or P8 infiltrated leaf patches were weaker compared to TriMV P1, suggesting that HPWMoV P7 and P8 are relatively weak in suppression of silencing in infiltrated leaf patches. To exclude the possibility of relatively weak silencing suppression activity of P7 and P8 is due to low levels of respective protein expression in infiltrated leaves, the hemagglutinin (HA) epitope was tagged at the N-terminus of P7 and P8 and ligated into pCASS4 under the 35S promoter. The level of P7 and P8 expression in agroinfiltrated *N. benthamiana* leaves with respective HA-tagged constructs was examined using a monoclonal antibody specific to the HA epitope. At 3 dpi, both P7 and P8 accumulated at similar levels to that of TriMV P1, a strong suppressor of RNA silencing (Tatineni et al., 2012; Fig. 1D), indicating that relatively weak silencing suppression activity of P7 and P8 is not due to low levels of protein expression or stability. As a negative control, HA-tagged HPWMoV P3 failed to accumulate at detectable levels in *N. benthamiana* leaf patches due to RNA silencing (Fig. 1D).

2.2. Both P7 and P8 suppress dsRNA-induced silencing

Double-stranded RNA is a strong inducer of RNA silencing compared to single-stranded RNA (Fire et al., 1998). To examine the efficiency of P7 and P8 in suppressing dsRNA-induced RNA silencing, agrobacteria with 35S-dsGFP (Tatineni et al., 2012) and 35S-GFP (reporter gene) were co-infiltrated with pCASS-P3, -P7 or -P8 into *N. benthamiana* leaves. At 2 dpi, green fluorescence was observed in leaf patches infiltrated with P7, P8, or TriMV P1, and was completely silenced in P3 or pCASS4 infiltrated leaf patches (Fig. 2A). The levels of silencing suppression and silencing were assayed by northern blot hybridization with GFP-specific riboprobes. GFP mRNA was accumulated in P7, P8 or TriMV P1 infiltrated leaf patches at 1 and 2 dpi, but it was not found at detectable levels in leaf patches infiltrated with P3 or pCASS4 (Fig. 2B). Accumulation of siRNAs was significantly reduced in P7, P8 or TriMV P1 infiltrated leaf patches compared to large amounts of siRNAs accumulation in P3 or pCASS4 infiltrated leaf patches (Fig. 2B). These data further confirm that P7 and P8 are suppressors of RNA silencing of HPWMoV.

2.3. P7 and P8 suppress transitive pathway of RNA silencing

siRNAs guide silencing effectors such as RISC for target repression, and this can quickly cascade into an amplification phase that generates secondary or transitive siRNAs from the regions of primary site, resulting in enhanced RNA silencing both at the local and systemic level
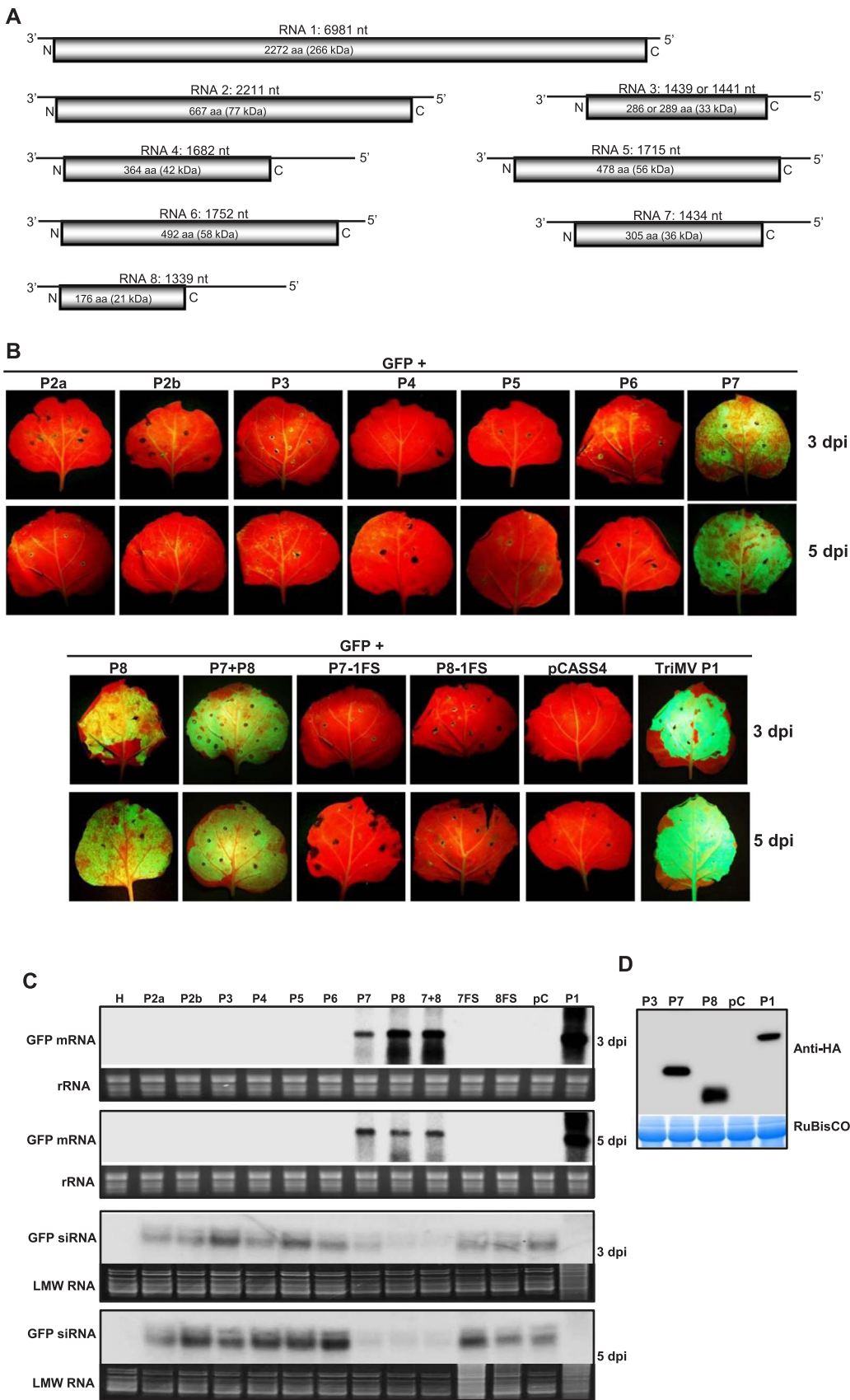
Fig. 1. HPWMoV P7 and P8 suppress local RNA silencing induced by single-stranded GFP mRNA. (A) Genome organization of octapartite single-stranded negative-sense RNAs of HPWMoV. The schematic representation of each of genomic RNA species is presented with an encoded ORF (open rectangles) with 3′ and 5′ non-translated regions. The number of amino acids and molecular weight of proteins encoded by each genomic RNA species are indicated. (B) Green fluorescent images of *Nicotiana benthamiana* leaves infiltrated with agrobacterial suspension harboring pCASS4 containing individual HPWMoV ORFs and 35S-GFP, as indicated above leaf images. pCASS-TriMV P1 and empty pCASS4 were used as positive and negative controls, respectively. Note the GFP fluorescence in leaves infiltrated with P7, P8, or P7 + P8 but not with other HPWMoV-encoded proteins. (C) Northern blot hybridization analysis of total RNA from agroinfiltrated leaf patches for GFP-specific mRNA (top two panels) and siRNA accumulation (bottom two panels). Ethidium bromide stained gels in top two and bottom two panels showing the 28S rRNA and low molecular weight (LMW) RNA, respectively, for the amount of total RNA loaded per well. (D) Western blot assay showing accumulation of HA-tagged proteins at 3 dpi. Bottom panel shows the Coomassie Brilliant Blue R-250 stained RuBisCO protein to represent the amount of protein loaded per well. dpi: days postinfiltration.

(Melnyk et al., 2011). Most RNA silencing suppressors are known to block either local silencing, or systemic silencing, or both (Hamilton et al., 2002). To determine whether P7 and P8 can suppress systemic silencing by blocking the mobile inducers of RNA silencing, we coinfiltrated an *Agrobacterium* suspension harboring 35S-GFP with pCASS-P3, -P7, or -P8 into the leaves of GFP transgenic *N. benthamiana* line 16c
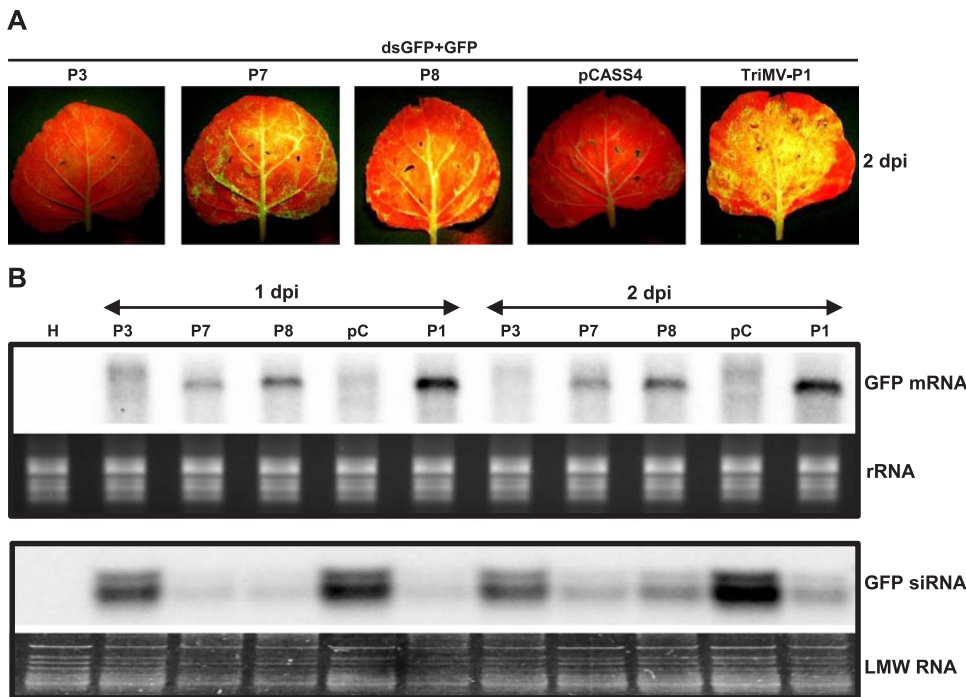
A

B

Fig. 2. HPWMoV P7 and P8 suppress local silencing induced by GFP double-stranded (ds) RNA. (A) Fluorescent images of agroinfiltrated *N. benthamiana* leaves with a combination of three constructs as indicated. (B) Northern blot analyses of total RNA from agroinfiltrated leaf patches for accumulation of GFP mRNA (top panel) and GFP-specific siRNA (bottom panel) at 1 and 2 dpi. Ethidium bromide stained gels showing rRNA (top panel) and low molecular weight (LMW) RNAs (bottom panel) for the amount of total RNA loaded per well. dpi: days postinfiltration.

at the 6–8-leaf stage as depicted in Fig. 3A, i. At 15 dpi, agroinfiltrated plants were examined under UV illumination for systemic silencing in the upper noninfiltrated leaves (Fig. 3B). Plants infiltrated with agro-suspension harboring 35S-GFP + pCASS-P7 or -P8 resulted in no systemic silencing (0/40 plants). In contrast, 38–40 of 40 agroinfiltrated plants (95–100%) were systemically silenced with 35S-GFP + pCASS-P3 or pCASS4 (Fig. 3C, group i). These results indicate that HPWMoV P7 and P8 suppress the transitive pathway of RNA silencing.

We next examined whether P7 and P8 can block the movement of silencing inducers from the site of infiltration by agroinfiltrating 35S-GFP and pCASS-P3, -P7, -P8, or pCASS4 separately into *N. benthamiana* line 16c leaves (Fig. 3A). *Agrobacterium*-suspension harboring 35S-GFP was infiltrated into bottom leaves, while pCASS-P3, -P7, -P8, or pCASS4 was infiltrated into the top leaves (Fig. 3A, ii). In another set, agro-suspension harboring pCASS-P3, -P7, -P8, or pCASS4 was infiltrated into bottom leaves, while 35S-GFP was infiltrated into top leaves (Fig. 3A, iii). At 15 dpi, plants infiltrated with P7 or P8 into the top leaves showed 0% systemic silencing, and P3 or pCASS4 infiltrated plants exhibited 100% systemic silencing (Fig. 3C, group ii). In contrast, plants infiltrated with P7 or P8 in bottom leaves and GFP infiltrated in top leaves systemically silenced 100% of plants similar to those of P3 or pCASS4 (Fig. 3C, group iii). These data suggest that P7 and P8 efficiently suppressed transient silencing by blocking systemic spread of silencing inducing signals toward the top leaves. These data also confirm that P7 and P8 suppress RNA silencing after production of silencing signals.

2.4. P7 and P8 independently rescue a heterologous virus lacking suppressor of RNA silencing

Previously, we have reported that P1 of *Wheat streak mosaic virus* (WSMV; genus *Tritimovirus*; family *Potyviridae*), a wheat infecting virus, is a strong suppressor of RNA silencing (Young et al., 2012). Recently, we developed a GFP-tagged WSMV for efficient tracking of the virus in wheat (Tatineni et al., 2011, 2014b). The RNA silencing suppression activity of HPWMoV P7 and P8 was further confirmed by examining whether P7 and P8 would rescue the P1-deficient WSMV mutant. The P1 cistron of WSMV was precisely replaced with that of P7 or P8 ORF of HPWMoV in pSP6-WSMV-GFP-6K1/CI(7aa) (Tatineni et al., 2011) to

obtain pWSMV-ΔP1-GFP-P7 and pWSMV-ΔP1-GFP-P8, respectively (Fig. 4A). As negative controls, the P1 cistron of WSMV was deleted (pWSMV-ΔP1-GFP) and also replaced with the P3 ORF of HPWMoV (pWSMV-ΔP1-GFP-P3) (Fig. 4A). The eleven amino acid NIa-Pro cleavage peptide located between the NIb and CP cistrons of WSMV (heptapeptide with two spacer amino acids on either side) was fused to the C-terminus of P3, P7, and P8 ORFs before replacing the P1 cistron in WSMV-GFP. The capped *in vitro* transcripts of GFP-tagged WSMV mutants lacking P1 but harboring HPWMoV P3, P7, or P8 and WSMV-ΔP1-GFP were mechanically inoculated onto 15–20 wheat seedlings at the single-leaf stage. Wheat leaves were examined under a Zeiss Stereo Discovery V12 fluorescence dissecting microscope (Carl Zeiss Micro-Imaging, Inc., New York) for the development of local foci and systemic infection at 7 and 21 days after-inoculation (dai), respectively. WSMV-ΔP1-GFP-P7 and WSMV-ΔP1-GFP-P8 elicited 4–5 foci per leaf, but no foci were detected in wheat leaves inoculated with WSMV-ΔP1-GFP-P3 or WSMV-ΔP1-GFP (Fig. 4B; Table 1). Wild-type WSMV-GFP [WSMV-GFP-6K1/CI(7aa)] elicited 8 foci per leaf on inoculated leaves of wheat. Fluorescent foci elicited by WSMV-ΔP1-GFP-P7 or WSMV-ΔP1-GFP-P8 were not as bright as those of wild-type WSMV-GFP (Fig. 4B, top panel), suggesting that P1-deficient WSMV with HPWMoV P7 or P8 might be replicating at reduced levels compared to wild-type virus.

At 21 dpi, upper uninoculated leaves of wheat were examined under a fluorescence microscope for systemic infection. Wheat inoculated with wild-type WSMV-GFP infected 80% of plants systemically and GFP fluorescence covered the entire leaf lamina (Fig. 4B, bottom panel; Table 1). WSMV-ΔP1-GFP-P7 or WSMV-ΔP1-GFP-P8 systemically infected 40–50% of the plants (Table 1), but fluorescence was mostly restricted to veins, except in a few leaves where fluorescence covered most of the leaf lamina (Fig. 4B, bottom panel). This demonstrates that HPWMoV P7 and P8 rescued the RNA silencing suppressor-deficient WSMV mutant. Wheat inoculated with WSMV-ΔP1-GFP-P3 or WSMV-ΔP1-GFP failed to infect systemically as no detectable GFP fluorescence was observed in upper uninoculated leaves.

Viral infection was further confirmed through RT-PCR amplification of the WSMV CP cistron from total RNA extracted from inoculated and upper uninoculated leaves at 7 and 21 dai, respectively. For both 7 and 21 dai sampling, a DNA band of 1.2 kbp was obtained from WSMV-GFP, WSMV-ΔP1-GFP-P7, and WSMV-ΔP1-GFP-P8 but not from WSMV-ΔP1-

A

B

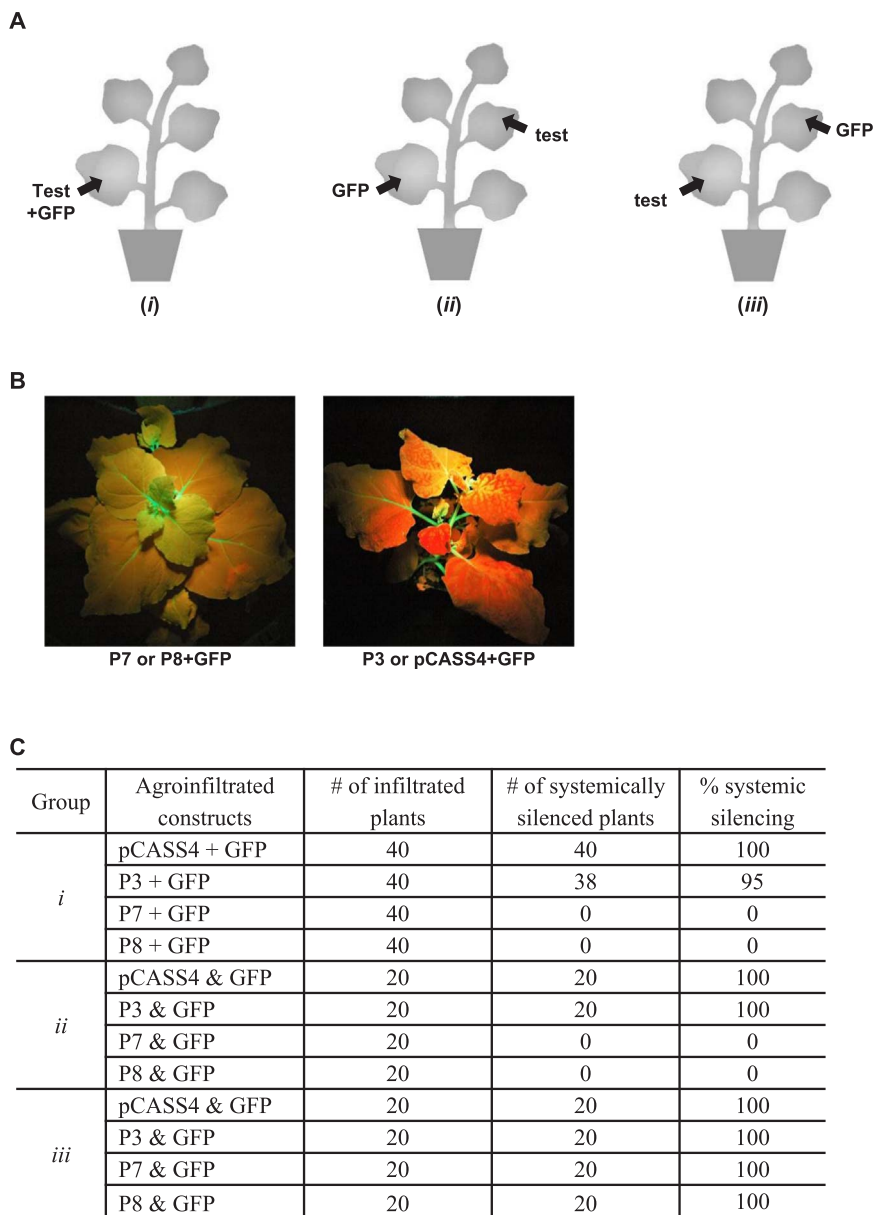P7 or P8+GFP   P3 or pCASS4+GFP

Fig. 3. HPWMoV P7 and P8 suppress transitive pathway of RNA silencing by blocking silencing signals. (A) Schematic diagrams of positions of infiltrated leaves of GFP-transgenic *N. benthamiana* line 16c plants with agrobacterial suspension harboring select HPWMoV ORFs (test) and 35S-GFP (GFP) as indicated. P3, P7, or P8 was included as test constructs coinfiltrated with 35S-GFP (group i), 35S-GFP infiltrated in lower leaves and the test constructs in upper leaves (group ii), and test constructs infiltrated in lower leaves and 35S-GFP in upper leaves (group iii). (B) Agroinfiltrated *N. benthamiana* line 16c plants under UV illumination showing no silencing (infiltrated with P7 or P8 + 35S-GFP) and systemic silencing (infiltrated with P3 or pCASS4 + 35S-GFP) at 15 dpi. GFP-transgenic *N. benthamiana* line 16c plants were infiltrated at the six-leaf stage. (C) Systemic silencing of GFP in *N. benthamiana* line 16c agroinfiltrated with test constructs plus 35S-GFP in group i, ii, and iii plants as shown in 'A'. Two to four independent experiments were conducted with 10 plants per experiment.

C

Group	Agroinfiltrated constructs	# of infiltrated plants	# of systemically silenced plants	% systemic silencing
i	pCASS4 + GFP	40	40	100
	P3 + GFP	40	38	95
	P7 + GFP	40	0	0
	P8 + GFP	40	0	0
ii	pCASS4 & GFP	20	20	100
	P3 & GFP	20	20	100
	P7 & GFP	20	0	0
	P8 & GFP	20	0	0
iii	pCASS4 & GFP	20	20	100
	P3 & GFP	20	20	100
	P7 & GFP	20	20	100
	P8 & GFP	20	20	100

GFP-P3 or WSMV-ΔP1-GFP (Fig. 4C, primer set I). An additional RT-PCR was performed on the same RNA samples with primers flanking WSMV P1 to examine the stability of HPWMoV P7 and P8 ORFs in WSMV genome in infected wheat. PCR products with sizes of 1.6, 1.5 and 1.2 kbp were obtained from wheat infected with WSMV-GFP, WSMV-ΔP1-GFP-P7, or WSMV-ΔP1-GFP-P8, respectively (Fig. 4C, primer set II, lanes 1, 4 and 5), indicating WSMV stably maintained the HPWMoV sequences. No RT-PCR product was obtained from wheat inoculated with WSMV-ΔP1-GFP-P3 or WSMV-ΔP1-GFP (Fig. 4C, primer set II, lanes 2 and 3), as there was no establishment of infection due to lack of suppressor of RNA silencing.

Western blot was performed with a monoclonal antibody and polyclonal antisera against GFP and WSMV CP, respectively, on total protein extracted from upper uninoculated leaves at 21 dai (Fig. 4D). A 30 kDa protein was detected with a GFP monoclonal antibody from systemic leaves of wheat inoculated with WSMV-GFP, WSMV-ΔP1-GFP-P7, or WSMV-ΔP1-GFP-P8, but not from WSMV-ΔP1-GFP-P3 or WSMV-ΔP1-GFP inoculated wheat (Fig. 4D, upper panel). Western blot with WSMV CP antibodies revealed accumulation of a major protein of 45 kDa and two minor proteins of 32 and 29 kDa proteins (Tatineni and

French, 2014) from wheat inoculated with wild-type virus or WSMV-ΔP1-GFP with HPWMoV P7 or P8 but not with WSMV-ΔP1-GFP-P3 or WSMV-ΔP1-GFP (Fig. 4D, middle panel). Accumulation of GFP and WSMV CP in wheat infected by WSMV-ΔP1-GFP-P7 or -P8 was 10–12-fold lower compared with wild-type WSMV-GFP [Fig. 4D, compare lane 1 (1:10 dilution) with lanes 4 and 5]. This further confirmed reduced levels of replication of WSMV-ΔP1-GFP with HPWMoV P7 or P8. Taken together, these data confirm that HPWMoV P7 and P8 ORFs rescued a silencing suppressor-deficient WSMV mutant for replication and cell-to-cell and long-distance movement in wheat.

2.5. P7 and P8 enhance pathogenicity of a heterologous virus

Most suppressors of RNA silencing have been shown to synergistically enhance the severity of infection when chimerically expressed through heterologous viruses (Cañizares et al., 2008; Cao et al., 2005; Samuel et al., 2016; Tatineni et al., 2012). To test this hypothesis, we used a recombinant *Potato virus X* (PVX) to express HPWMoV P3, P7, or P8 ORFs in *N. benthamiana*. Sequences encoding for P3, P7 and P8 ORFs of HPWMoV were amplified by RT-PCR from virion RNA and inserted
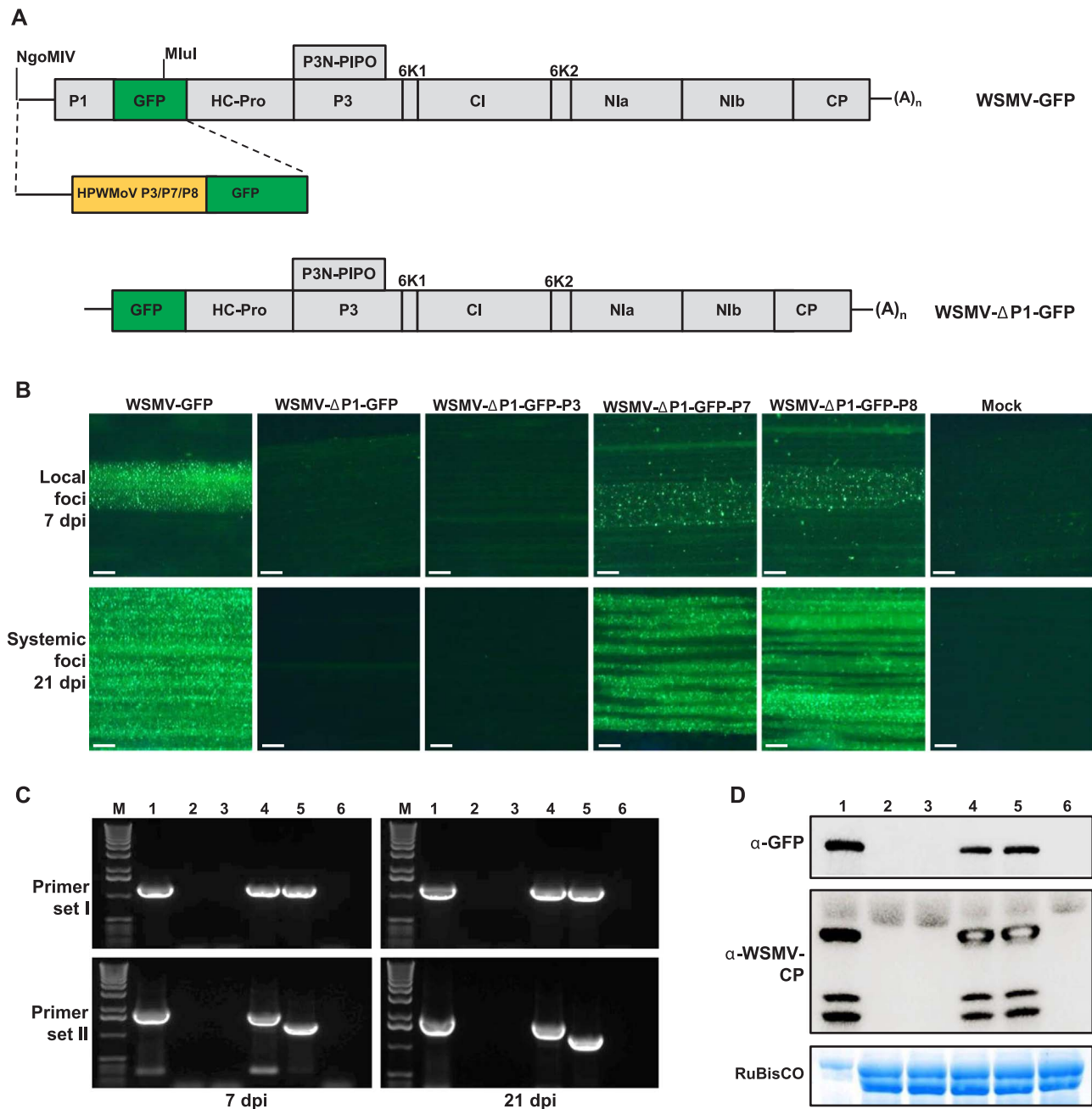
Fig. 4. HPWMoV P7 and P8 independently rescue a *Wheat streak mosaic virus* (WSMV) mutant lacking the suppressor of RNA silencing. (A) Schematic representation of genomic organizations of WSMV-GFP and WSMV-ΔP1-GFP with encoded proteins indicated. The expanded view of 5′ region of WSMV-GFP with P1 replaced with that of HPWMoV P3, P7, or P8 ORFs is indicated below the genomic organization of WSMV-GFP. A line between HPWMoV ORFs and GFP indicates the engineered 11 amino acid NIa-Pro cleavage peptide located between the NIb/CP cistrons. The location of *NgoM*IV and *Mlu*I restriction sites used for replacing the WSMV P1 cistron with overlap extension PCR products comprising the P3, P7, or P8 ORFs of HPWMoV are indicated. (B) Fluorescent micrographs showing GFP expression in inoculated (top panel) and upper uninoculated leaves (bottom panel) of wheat by GFP-tagged viruses as indicated. The scale bars represent 200 µm. (C) Diagnostic RT-PCR of WSMV CP (top panel) and with primers flanking on either side of WSMV P1 (bottom panel) from the total RNA extracted from inoculated wheat leaves at 7 (left panels) dai and upper uninoculated leaves at 21 dai (right panels). Wheat inoculated with WSMV-GFP (lane 1), WSMV-ΔP1-GFP (lane 2), WSMV-ΔP1-GFP-P3 (lane 3), WSMV-ΔP1-GFP-P7 (lane 4), WSMV-ΔP1-GFP-P8 (lane 5) and mock (lane 6) were used for total RNA extraction. Lane M represents 1.0 kbp DNA ladder. (D) Western blot analyses on total protein extracted from upper uninoculated leaves at 21 dai from samples as indicated in 'C' with anti-GFP monoclonal antibody (top panel) and anti-WSMV-CP polyclonal antibodies (middle panel). Bottom panel shows Coomassie Brilliant Blue R-250 stained SDS-PAGE showing the RuBisCO protein for the amount of protein loaded per well. Total protein from WSMV-GFP-infected wheat was loaded at 1:10 dilution in lane 1. Dai: days after-inoculation.

into pP2C2S-PVX (Chapman et al., 1992) to obtain pPVX-P3, pPVX-P7, and pPVX-P8, respectively. *In vitro* transcripts from pPVX constructs were mechanically inoculated onto two fully expanded upper leaves of *N. benthamiana* at the 6–8 leaf stage. At 12–14 dai, all PVX constructs elicited systemic mosaic and mottling, followed by inward leaf curling. However, at 18–21 dai, PVX expressing P7 or P8 caused stunted growth with severe leaf curling compared with veinal chlorosis and mosaic symptoms elicited by PVX-P3 and PVX. At 28 dai, PVX-P7 inoculated *N.*

benthamiana showed severe stunting with necrotic spots and apical necrosis, while PVX-P8 inoculated plants also showed similar symptoms but with milder apical necrosis (Fig. 5A). At 28 dai, systemic symptoms on PVX-P3- or PVX-inoculated plants showed milder mosaic and mottling (Fig. 5A).

To correlate the relationship between disease severity and viral accumulation, we performed quantitative real-time RT-PCR (qRT-PCR) on each sample in duplicate at 21 and 28 dai. Nonspecific basal

Table 1
Number of local foci and systemically infected wheat plants by GFP-tagged silencing suppressor-deficient *Wheat streak mosaic virus* harboring P7 or P8 ORFs of HPWMoV.

Virus	Average # of local foci per leaf[b]	Systemic infection[c]		
		# of plants inoculated	# of plants infected	% infection
WSMV-GFP (WT)	7.1 ± 0.8	20	16	80
WSMV-ΔP1[a]-GFP	0	15	0	0
WSMV-ΔP1-GFP-P3	0	15	0	0
WSMV-ΔP1-GFP-P7	3.4 ± 0.8	24	10	41.6
WSMV-ΔP1-GFP-P8	4.8 ± 0.8	22	11	50
Mock	0	14	0	0

WT: Wild-type virus; P3: HPWMoV P3 open reading frame (ORF).
  [a] P1 is the suppressor of RNA silencing of WSMV (Young et al., 2012).
  [b] Local foci counted under Zeiss Stereo Discovery V12 fluorescence microscope on inoculated leaves at 7 days after inoculation (dai).
  [c] The upper uninoculated leaves of wheat were observed for systemic foci under a fluorescence microscope at 21 dai.

expression from mock-inoculated plants was subtracted from each infected sample. The relative expression of PVX was calculated by normalizing with an internal reference of *Nb* Actin expression by ΔΔCt method (Bustin et al., 2009) (Fig. 5B). The relative expression of PVX-P7 revealed 16- and 27-fold increase, and PVX-P8 exhibited 11- and 24-fold increase at 21 and 28 dai, respectively, compared to wild-type PVX. However, accumulation of PVX-P3 in *N. benthamiana* at 21 and 28 dai was similar to wild-type PVX (Fig. 5B). These data suggest that HPWMoV P7 and P8 significantly enhanced pathogenicity of PVX by increasing virus accumulation in *N. benthamiana*. To confirm stability of the inserts, RT-PCR was performed on total RNA extracted from symptomatic leaf tissue at 28 dai, by using primers flanking the site of insertion. RT-PCR amplification obtained expected products from *N. benthamiana* infected with PVX harboring HPWMoV sequences (Fig. 5C), suggesting that PVX stably retained the HPWMoV sequences until 28 dai.

3. Discussion

Viruses have evolved by encoding one or more suppressors of RNA silencing to counteract host defense mechanisms (Csorba et al., 2015; Li and Ding, 2006). In this study, we report that the octapartite negative-sense RNA genome of HPWMoV, an accepted species of the genus *Emaravirus*, encodes two suppressors of RNA silencing. HPWMoV P7 and P8 suppressed GFP-induced local silencing and the transitive pathway of silencing, and dramatically increased symptom phenotype of PVX in *N. benthamiana*. Importantly, P7 and P8 proteins independently rescued the silencing suppressor-deficient mutant of heterologous wheat-infecting WSMV. In this study, we did not examine HPWMoV RNA 1 for potential RNA silencing suppression function. However, RNA 1 encodes for replication-associated proteins, thus it is unlikely that RNA 1 encodes a domain with suppression of RNA silencing activity.

Screening of HPWMoV encoded ORFs 2–8 using the GFP reporter assay for suppression of ssRNA- and dsRNA-induced local silencing revealed that proteins encoded by RNA 7 (P7) and 8 (P8), but not their RNAs, suppressed local silencing. Under the same experimental conditions, P7 and P8 suppressed local silencing weakly compared to that of P1 of TriMV (Tatineni et al., 2012). The level of suppression of RNA silencing by P7 and P8, either independently or together, was similar (Fig. 1B, C), suggesting that P7 and P8 proteins might target the same pathway of host defense at the cellular level. The weak nature of suppression of local silencing of P7 and P8 could be due to their inherent characteristic of suppression of RNA silencing. Analyses of total RNA from agroinfiltrated leaf patches revealed that P7 and P8 caused a substantial reduction in siRNA accumulation. These data suggest that P7 and P8 did not affect the biogenesis of siRNAs but they may act downstream of siRNA biogenesis. Perhaps P7 and P8 sequester the already silenced transgene to hamper further amplification as shown with

a tombusvirus p19 (Silhavy et al., 2002).

In contrast to relatively weak suppression of RNA silencing at the cellular level, both P7 and P8 efficiently suppressed the transitive pathway of silencing. The mobile signals of silencing induction on their systemic route through the vasculature render enhanced systemic defense against existing replicating viruses as well as superinfections by related viruses (Voinnet and Baulcombe, 1997). However, in the absence of a potential silencing suppressor, the siRNAs derived from a transgene would move uninterrupted to upper portion of plants through the vasculature effecting transitive silencing of the transgene in upper uninoculated leaves. Systemic silencing was efficiently suppressed when P7 or P8 was co-infiltrated with 35S-GFP, or P7 or P8 was infiltrated in upper leaves but not in the lower leaves compared to 35S-GFP (silencing inducer). These data suggest that P7 and P8 expressed in upper leaves efficiently blocked the mobile signals of RNA silencing from reaching the top leaves, thereby suppressing the transitive pathway of RNA silencing. Since P7 and P8 did not inhibit biogenesis of siRNAs, these data suggest that P7 and P8 physically bind to siRNAs at the interface, thus preventing the systemic spread of siRNAs to upper young leaves (Guo and Ding, 2002; Lakatos et al., 2006). However, further experiments are needed to unravel the mechanisms of suppression of RNA silencing by HPWMoV P7 and P8.

The suppression of RNA silencing activity of unknown viral genes was demonstrated by agroinfiltration assay (Llave et al., 2000) or expression through a heterologous virus for increased pathogenicity (Myles et al., 2008; Pruss et al., 1997; Samuel et al., 2016). Systemic infection of *Plum pox virus* was supported by a few heterologous RNA silencing suppressors (Maliogka et al., 2012), suggesting that rescue of RNA silencing suppressor-deficient viruses with candidate genes could provide evidence for their RNA silencing suppression activity. In this study, we used the replace-a-gene strategy by precisely replacing the P1 cistron, the suppressor of RNA silencing of WSMV (Young et al., 2012), with that of HPWMoV P7 or P8 ORF in a GFP-tagged WSMV. A WSMV-GFP mutant lacking P1, but having either P7 or P8 from HPWMoV, facilitated cell-to-cell and long-distance movement in wheat, thus rescuing the loss of the WSMV silencing suppressor function. These data further support that P7 and P8 are RNA silencing suppressors of HPWMoV. Since P7 and P8 similarly replaced P1's silencing suppression function in WSMVΔP1-GFP and no significant additive effect of P7 and P8 in coinfiltrated leaves was found, it is possible that both HPWMoV silencing suppressors similarly target the host defense pathways. Though P1's silencing suppression function in WSMV-ΔP1-GFP was rescued with either P7 or P8, WSMV mutants with either of these ORFs accumulated at reduced levels compared to wild-type virus. These data suggest that either heterologous RNA silencing suppressors may not be fully compatible or P1 may also be involved in other functions of WSMV biology, such as efficient replication. Nonetheless, both suppressors of RNA silencing of a multipartite negative-sense RNA virus independently rescued a silencing suppressor-deficient monopartite positive-sense
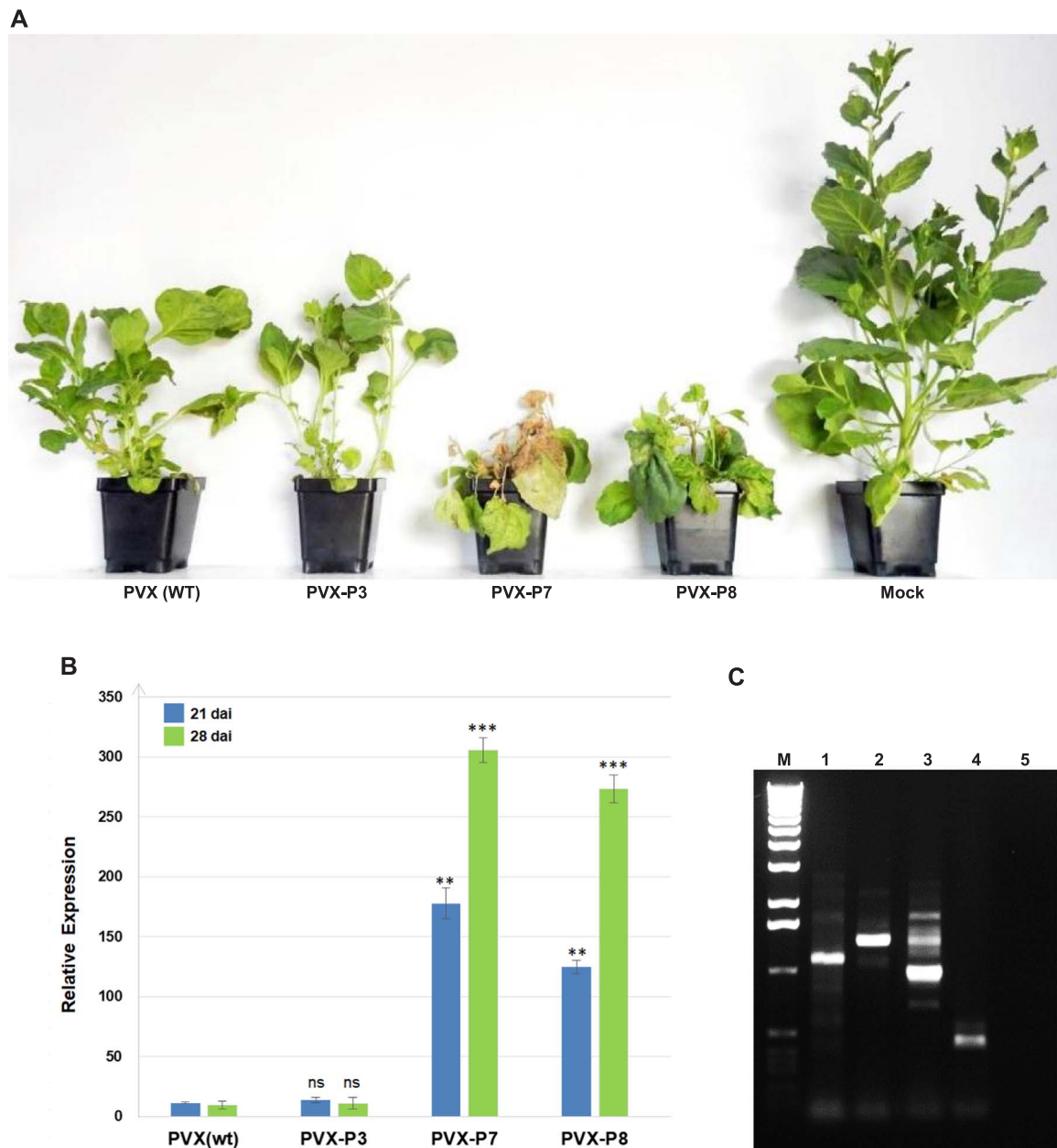
Fig. 5. RNA silencing suppressors of HPWMoV enhance pathogenicity of *Potato virus X* (PVX) in *Nicotiana benthamiana*. (A) Symptom phenotype of wild-type PVX and PVX with P3, P7, or P8 ORFs of HPWMoV in *N. benthamiana* at 28 days after-inoculation (dai). Note that PVX with P7 or P8 ORFs elicited severe symptoms in *N. benthamiana*. (B) Relative quantification of PVX genomic RNA in *N. benthamiana* plants infected with wild-type PVX, PVX-P3, PVX-P7, or PVX-P8. Relative expression of PXV was calculated by performing reverse-transcription real-time PCR from total RNA extracted from *N. benthamiana* plants infected by PVX and PVX expressing HPWMoV ORFs. Relative expression values were computed by ΔΔCt method using Nb-Actin as internal reference of expression for normalization. The error bars represent the standard error. Probability values for differences in accumulation of PVX genomic RNA copies in PVX-P3, -P7, and P8 infected plants over wild-type PVX was calculated using Student's *T*-Test. **, ***, and ns represent the confidence level at 95%, 99% and not significant, respectively. (C) RT-PCR analyses for the stability of inserts in upper symptomatic leaves of *N. benthamiana* plants inoculated with PVX-P3 (lane 1), PVX-P7 (lane 2), PVX-P8 (lane 3), wild-type PVX (lane 4), and mock (lane 5) at 28 dai. The forward and reverse primers were used for RT-PCR flanking the location of insertion in the PVX genome. Lane M: 1 kbp DNA ladder.

RNA virus.

Most of the suppressors of RNA silencing are also involved in pathogenicity enhancement, and the role of suppressors of RNA silencing in pathogenicity was demonstrated by expressing through heterologous viruses as expression vectors (Samuel et al., 2016; Tatineni et al., 2012). PVX with HPWMoV P7 or P8 caused significantly increased symptoms in *N. benthamiana*, suggesting that silencing suppressors of HPWMoV might have synergistically interacted with PVX. However, slight differences found in symptom phenotype of PVX with P7 or P8 suggest that these two proteins may differentially affect the miRNA pathway (Mallory et al., 2002). The dramatically increased symptom phenotype of PVX in *N. benthamiana* together with steady-state accumulation of

PVX genomic RNA suggests that HPWMoV P7 and P8 are also strong pathogenicity determinants. Recently, Lu et al. (2015) reported that P6 and P7 of RLBV also increased pathogenicity of PVX in *N. benthamiana*, but they were unable to provide evidence for RNA silencing suppression activity. It is possible that failure to identify a silencing suppressor encoded by the RLBV genome could be due to their weak silencing suppression activity at the cellular level, as observed with HPWMoV P7 and P8 (this study).

Plant viruses that encode more than one suppressors of RNA silencing have been reported in criniviruses, closteroviruses and geminiviruses (Cañizares et al., 2008; Lu et al., 2004; Vanitharani et al., 2004). Viral suppressors of RNA silencing display a remarkable functional

conservation with little or no sequence and structural conservation (Burgyan and Havelda, 2011). Thus, it is apparent that the existing or newly acquired genes might have become involved in counterdefensive function to overcome the host RNA silencing. Since HPWMoV P7 and P8 show no apparent sequence homology with other reported viral genes, it is possible that HPWMoV might have acquired these genes for suppression of RNA silencing, with possible other functions in virus biology. However, future experiments on the mechanisms of P7 and P8 to counter the host defense mechanisms could provide insights on suppressors of RNA silencing encoded by a plant virus with multipartite single-stranded negative-sense RNA genome.

4. Materials and methods

4.1. Generation of constructs

HPWMoV-Nebraska isolate virion RNA, prepared from partially purified nucleocapsids (Tatineni et al., 2014a), was used as a template for RT-PCR amplification of HPWMoV-encoded ORF 2a, 2b, 3A, and 4–8. The HPWMoV ORF-specific forward and reverse primers were synthesized based on GenBank sequence with accession numbers: KJ939624 (ORFs 2a and 2b), KJ939625 (ORF 3A), and KJ939627 to KJ939631 (ORFs 4–8). *Tobacco etch virus*-leader sequence (Carrington and Freed, 1990) was fused to the 5' end of each of HPWMoV ORF through overlap extension PCR (Ho et al., 1989) and ligated into pCASS4 between *Stu*I and *Sac*I restriction sites. pCASS-TriMV P1 and pPZP-dsGFP (35S-dsGFP), and pPZP-GFP (35S-GFP) were previously described in Tatineni et al. (2012) and Qu et al. (2003), respectively. Frameshift mutants (−1) of P7 and P8 were generated by deleting one nucleotide in the first codon of each ORF, followed by ligation into pCASS4 between *Stu*I and *Sac*I restriction sites. All PCR reactions were performed with Herculase II Fusion DNA polymerase (Agilent Technologies, Santa Clara, CA). The presence of authentic sequence in plasmid DNAs was confirmed by nucleotide sequencing using Applied Biosystems 3730xl DNA Analyzer at the University of Florida ICBR Core DNA Sequencing Facility.

4.2. GFP-reporter assays

pCASS4 with HPWMoV ORFs were chemically transformed into the *Agrobacterium tumefaciens* strain EHA105. Agrobacteria grown overnight was centrifuged at 4500*g* for 15 min at room temperature, and bacterial pellets were suspended in 10 mM $MgCl_2$ with 10 mM MES (pH 5.5) containing 100 µM Acetosyringone to an optical density of 1.0 at 600 nm, and incubated at room temperature for 3–4 h. Local silencing was assayed by mixing equal amount of *Agrobacterium* suspension harboring HPWMoV ORFs with those of 35S-GFP or 35S-GFP and 35S-dsGFP, followed by infiltration into fully expanded leaves of *N. benthamiana* at 6–8 leaf stage. For systemic silencing, *N. benthamiana* GFP transgenic line 16c plants (Voinnet and Baulcombe, 1997) were infiltrated with equal amounts of agrosuspension harboring pCASS-P3, -P7 or -P8 and 35S-GFP at 6 leaf stage. Infiltrated *N. benthamiana* plants were maintained at 24–26 °C with a 14 h photoperiod. GFP fluorescence was observed under a long-wavelength UV radiation (Black-Ray Model B-100A, San Gabriel, CA) and photographed through an orange filter with a digital SLR camera (Nikon D70, Melville, NY).

4.3. Northern hybridization

Total RNA was extracted from agroinfiltrated leaf tissue of *N. benthamiana* by using Tripure reagent as described in Tatineni et al. (2012). Two micrograms of total RNA was resolved through 1.0% agarose gels containing formaldehyde (for GFP mRNA) or 15% polyacrylamide-urea gels (for GFP siRNA) and electro-transferred onto positively charged nylon membranes (Roche, Indianapolis, IN). The blotted nylon membranes were hybridized with digoxigenin (DIG)-labeled antisense riboprobes for GFP specific mRNA or siRNA as described in Tatineni et al. (2012).

4.4. Rescue of RNA silencing suppressor-deficient WSMV

The P1 cistron of WSMV in pSP6-WSMV-GFP-6KI/CI (WSMV-GFP; Tatineni et al., 2011) was replaced with HPWMoV P3, P7 or P8 ORFs in pWSMV-ΔP1-GFP-P3, pWSMV-ΔP1-GFP-P7, and pWSMV-ΔP1-GFP-P8, respectively, through overlap extension PCR. For a negative control, WSMV-GFP lacking P1 (WSMV-GFP-ΔP1) was created by deleting sequence encoding the second through last codons of P1. *In vitro* transcription reactions were performed in a 40 µl reaction volume with 1.0 µg linearized plasmid DNA as described in Tatineni et al. (2011). Transcription reactions were mixed with an equal volume of 1% sodium pyrophosphate, pH 9.0 plus 1% baked celite, followed by rub inoculation onto wheat seedlings at the single-leaf stage. Inoculated wheat plants were maintained in a greenhouse at temperatures of 22–27 °C with a photoperiod of 16 h. Inoculated wheat leaves and fully expanded upper uninoculated leaves were examined at 7 and 21 dai, respectively, for GFP fluorescence using Zeiss Stereo Discovery V12 Fluorescence Microscope with a narrow-band GFP filter set 38 with 400–450 nm excitation and 450–490 nm emission. GFP fluorescent micrographs were captured with AxioCam MRc5 camera. Total RNA was extracted from inoculated and upper uninoculated leaves at 7 and 21 dai, respectively, by using the Tripure reagent method (Tatineni et al., 2012). Random primed cDNA was prepared from 1.0 µg of total RNA by using the SuperScript III First-Strand Synthesis System (Invitrogen, Carlsbad, CA), followed by PCR with oligonucleotides XV1 and XC1 (Tatineni et al., 2017) and W-479 (5′-GCTCTAGTTCAACAAAGTTCATCACG-3′, corresponding to nts 94–119 of WSMV-GFP) and W-481 (5′-AATTCAA CAAGAATTGGGACAACTCC-3′, complementary to nts 1276–1251 of WSMV-GFP).

4.5. Pathogenicity enhancement assay

HPWMoV P3, P7 and P8 ORFs were ligated into the PVX vector pP2C2S (Chapman et al., 1992) between *Cla*I and *Asc*I restriction sites. *In vitro* transcripts of PVX or PVX with HPWMoV ORFs were mechanically inoculated onto *N. benthamiana* at the 6–8-leaf stage and maintained in a growth chamber at 20 °C with a 16-h photoperiod. Total RNA was extracted from upper symptomatic leaves (400 mg) by using the TriPure method (Roche, Indianapolis, IN) at 21 and 28 dai. Random-primed cDNA from 1.0 µg each of total RNA was used for PCR with oligonucleotides Tr-206 (5′-GCACTTCCTTAGTGAGGACTGAAC CTT-3′, corresponding to nts 5494–5520 of PVX) and Tr-207 (5′-ATA GCCTCAATCTTGCTGAGGTCCTCA-3′, complementary to nts 5920–5894 of PVX).

4.6. Real-time RT-PCR

Real-time RT-PCR (qRT-PCR) was performed on total RNA extracted from *N. benthamiana* infected by wild-type PVX, PVX-P3, -P7, or -P8 at 21 and 28 dai. Two biological replicates in duplicate were used with the SsoAdvanced SYBR Green Supermix (Bio-Rad) in Bio-Rad CFX Connect Real-Time PCR System. qRT-PCR was performed with random primed cDNA with oligonucleotides G-35 (5′-ATGGATATTCTCATCATTAG-3′, corresponding to nts 4486–4505 of PVX) and G-36 (5′-CTATGTCCCT GCGCGGACATATG-3′, complementary to nts 5169–5147 of PVX). The following amplification conditions were used for qRT-PCR: 95 °C for 2 min followed by 40 cycles of 95 °C for 10 s, 55 °C for 30 s and 72 °C for 1 min qRT-PCR reactions without RNA template and reverse transcription were included as negative controls. Relative expression of PVX genomic RNA was computed by using the ΔΔCt method with an internal reference gene of *N. benthamiana* Actin used for normalization. Changes in the relative expression of PVX-P7 and -P8 were compared to that of wild-type PVX.

4.7. Western blot assay

Agroinfiltrated *N. benthamiana* leaves with HA-tagged HPWMoV P3, P7, P8, and TriMV-P1 in pCASS4 and an empty pCASS-HA at 3 dpi were homogenized in TPE buffer (50 mM Tris acetate; pH 7.4, 10 mM Potassium acetate, 1 mM EDTA, and 5 mM DTT) containing 1 Complete Mini Protease Inhibitor Cocktail tablet (Roche) per 10 ml of TPE buffer as described in Tatineni et al. (2011). Total proteins were also extracted from fully expanded upper leaves of wheat inoculated with WSMV-GFP and WSMV-ΔP1-GFP with HPWMoV P3, P7, or P8 ORFs at 21 dai in TPE buffer. Total proteins were subjected to sodium dodecyl sulfate-polyacrylamide gel electrophoresis through 4–20% gels (Invitrogen), and immunoblotting with a HA-specific monoclonal antibody (Sigma-Aldrich, St. Louis MO) (for HA-tagged proteins) or with a GFP-specific monoclonal antibody (Clontech Mountain View, CA) or WSMV polyclonal antisera (for GFP-tagged WSMV).

Acknowledgments

References

Aravin, A.A., Naumova, N.M., Tulin, A.V., Vagin, V.V., Rozovsky, Y.M., Gvozdev, V.A., 2001. Double-stranded RNA-mediated silencing of genomic tandem repeats and transposable elements in the D. melanogaster germline. Curr. Biol. 11, 1017–1027.

Bernstein, E., Caudy, A.A., Hammond, S.M., Hannon, G.J., 2001. Role for a bidentate ribonuclease in the initiation step of RNA interference. Nature 409, 363–366.

Bucher, E., Sijen, T., De Haan, P., Goldbach, R., Prins, M., 2003. Negative-strand tospoviruses and tenuiviruses carry a gene for a suppressor of gene silencing at analogous genomic positions. J. Virol. 77, 1329–1336.

Burgyan, J., Havelda, Z., 2011. Viral suppressors of RNA silencing. Trends Plant Sci. 16, 265–272.

Bustin, S.A., Benes, V., Garson, J.A., Hellemans, J., Huggett, J., Kubista, M., Mueller, R., Nolan, T., Pfaffl, M.W., Shipley, G.L., Vandesompele, J., Wittwer, C.T., 2009. The MIQE guidelines: minimum information for publication of quantitative real-time PCR experiments. Clin. Chem. 55, 611–622.

Cañizares, M.C., Navas-Castillo, J., Moriones, E., 2008. Multiple suppressors of RNA silencing encoded by both genomic RNAs of the crinivirus, Tomato chlorosis virus. Virology 379, 168–174.

Cao, X., Zhou, P., Zhang, X., Zhu, S., Zhong, X., Xiao, Q., Ding, B., Li, Y., 2005. Identification of an RNA silencing suppressor from a plant double-stranded RNA virus. J. Virol. 79, 13018–13027.

Carrington, J.C., Freed, D.D., 1990. Cap-independent enhancement of translation by a plant potyvirus nontranslational region. J. Virol. 64, 1590–1597.

Chapman, S., Kavanagh, T., Baulcombe, D.C., 1992. Potato virus X as a vector for gene expression in plants. Plant J. 2, 549–557.

Cogoni, C., Macino, G., 2000. Posttranscriptional gene silencing across kingdoms. Curr. Opin. Genet. Dev. 10, 638–643.

Csorba, T., Kontra, L., Burgyan, J., 2015. Viral silencing suppressors: tools forged to fine-tune host-pathogen coexistence. Virology 479–480, 85–103.

Ding, S.W., 2010. RNA-based antiviral immunity. Nat. Rev. Immunol. 10, 632–644.

Ding, S.W., Voinnet, O., 2007. Antiviral immunity directed by small RNAs. Cell 130, 413–426.

Fang, Y., Zhao, J., Liu, S., Wang, S., Duan, C., Guo, H., 2016. CMV2b-AGO interaction is required for the suppression of RDR-dependent antiviral silencing in Arabidopsis. Front. Microbiol. 7, 1329.

Fire, A., Xu, S., Montgomery, M., Kostas, S., Driver, S., Mello, C., 1998. Potent and specific genetic interference by double-stranded RNA in *Caenorhabditis elegans*. Nature 391, 806–811.

Fukudome, A., Kanaya, A., Egami, M., Nakazawa, Y., Hiraguri, A., Moriyama, H., Fukuhara, T., 2011. Specific requirement of DRB4, a dsRNA-binding protein, for the in vitro dsRNA-cleaving activity of Arabidopsis Dicer-like 4. RNA 17, 750–760.

Guo, H., Song, X., Xie, C., Huo, Y., Zhang, F., Chen, X., Geng, Y., Fang, R., 2013. Rice yellow stunt rhabdovirus protein 6 suppresses systemic RNA silencing by blocking RDR6-mediated secondary siRNA synthesis. Mol. Plant-Microbe Interact. 26, 927–936.

Guo, H.S., Ding, S.W., 2002. A viral protein inhibits the long range signaling activity of the gene silencing signal. EMBO J. 21, 398–407.

Haasnoot, J., de Vries, W., Geutjes, E.J., Prins, M., de Haan, P., Berkhout, B., 2007. The Ebola virus VP35 protein is a suppressor of RNA silencing. PLoS Pathog. 3 (6), e86.

Hammond, S.M., Bernstein, E., Beach, D., Hannon, G.J., 2000. An RNA-directed nuclease mediates post-transcriptional gene silencing in Drosophila cells. Nature 404, 293–296.

Hamilton, A.J., Baulcombe, D.C., 1999. A species of small antisense RNA in post-transcriptional gene silencing in plants. Science 286, 950–952.

Hamilton, A.J., Voinnet, O., Chappell, L., Baulcombe, D.C., 2002. Two classes of short interfering RNA in RNA silencing. EMBO J. 21, 4671–4679.

Ho, S.N., Hunt, H.D., Horton, R.M., Pullen, J.K., Pease, L.R., 1989. Site-directed mutagenesis by overlap extension using polymerase chain reaction. Gene 77, 51–59.

Holoch, D., Moazed, D., 2015. Small-RNA loading licenses Argonaute for assembly into a transcriptional silencing complex. Nat. Struct. Mol. Biol. 22, 328–335.

ICTV Report, 2016. Available online: ⟨https://talk.ictvonline.org/files/master-species-lists/m/msl/6776⟩.

Ishikawa, K., Maejima, K., Komatsu, K., Netsu, O., Keima, T., Shiraishi, T., Okano, Y., Hashimoto, M., Yamaji, Y., Namba, S., 2013. Fig mosaic emaravirus p4 protein is involved in cell-to-cell movement. J. Gen. Virol. 94, 682–686.

Ketting, R.F., Fischer, S.E., Bernstein, E., Sijen, T., Hannon, G.J., Plasterk, R.H.A., 2001. Dicer functions in RNA interference and in synthesis of small RNA involved in developmental timing in Caenorhabditis elegans. Genes Dev. 15, 2654–2659.

Lakatos, L., Csorba, T., Pantaleo, V., Chapman, E.J., Carrington, J.C., Liu, Y.-P., Dolja, V.V., Calvino, L.F., Lopez-Moya, J.J., Burgyán, J., 2006. Small RNA binding is a common strategy to suppress RNA silencing by several viral suppressors. EMBO J. 25, 2768–2780.

Li, F., Ding, S.W., 2006. Virus counter defense: diverse strategies for evading the RNA-silencing immunity. Annu. Rev. Microbiol. 60, 503–531.

Li, W.X., Li, H., Lu, R., Li, F., Dus, M., Atkinson, P., Brydon, E.W., Johnson, K.L., Garcia-Sastre, A., Ball, L.A., Palese, P., Ding, S.W., 2004. Interferon antagonist proteins of influenza and vaccinia viruses are suppressors of RNA silencing. Proc. Natl. Acad. Sci. USA 101, 1350–1355.

Llave, C., Kasschau, K.D., Carrington, J.C., 2000. Virus-encoded suppressor of post-transcriptional gene silencing targets a maintenance step in the silencing pathway. Proc. Natl. Acad. Sci. USA 97, 13401–13406.

Louie, R., Seifers, D.L., Bradfute, O.E., 2006. Isolation, transmission and purification of the High Plains virus. J. Virol. Methods 135, 214–222.

Lu, Y., McGavin, W., Cock, P., Schnettler, E., Yan, F., Chen, J., MacFarlane, S., 2015. Newly identified RNAs of Raspberry leaf blotch virus encoding a related group of proteins. J. Gen. Virol. 96, 3432–3439.

Lu, R., Maduro, M., Li, F., Li, H.W., Broitman-Maduro, G., Li, W.X., Ding, S.W., 2005. Animal virus replication and RNAi-mediated antiviral silencing in *Caenorhabditis elegans*. Nature 436, 1040–1043.

Lu, R., Folimonov, A., Shintaku, M., Li, W.X., Falk, B.W., Dawson, W.O., Ding, S.W., 2004. Three distinct suppressors of RNA silencing encoded by a 20-kb viral RNA genome. Proc. Natl. Acad. Sci. USA 101, 15742–15747.

Maliogka, V., I., Calvo, M., Carbonell, A., Garcia, J.A., Valli, A., 2012. Heterologous RNA-silencing suppressors from both plant- and animal-infecting viruses support Plum pox virus infection. J. Gen. Virol. 93, 1601–1611.

Mallory, A.C., Reinhart, B.J., Bartel, D., Vance, V.B., Bowman, L., 2002. A viral suppressor of RNA silencing differentially regulates the accumulation of short interfering RNAs and micro-RNAs in tobacco. Proc. Natl. Acad. Sci. USA 99, 15228–15233.

Mann, K.S., Johnson, K.N., Dietzgen, R.G., 2015. Cytorhabdovirus phosphoprotein shows RNA silencing suppressor activity in plants, but not in insect cells. Virology 476, 413–418.

Melnyk, C.W., Molnar, A., Baulcombe, D.C., 2011. Intercellular and systemic movement of RNA silencing signals. EMBO J. 30, 3553–3563.

Mérai, Z., Kerényi, Z., Kertész, S., Magna, M., Lakatos, L., Silhavy, D., 2006. Double-stranded RNA binding may be a general plant RNA viral strategy to suppress RNA silencing. J. Virol. 80, 5747–5756.

Mielke-Ehret, N., Mühlbach, H.P., 2012. Emaravirus: a novel genus of multipartite, negative strand RNA plant viruses. Viruses 4, 1515–1536.

Moazed, D., 2009. Small RNAs in transcriptional gene silencing and genome defence. Nature 457, 413–420.

Myles, K.M., Wiley, M.R., Morazzani, E.M., Adelman, Z.N., 2008. Alphavirus-derived small RNAs modulate pathogenesis in disease vector mosquitoes. Proc. Natl. Acad. Sci. USA 105, 1938–19943.

Park, W., Li, J., Song, R., Messing, J., Chen, X., 2002. CARPEL FACTORY, a Dicer homolog, and HEN1, a novel protein, act in microRNA metabolism in Arabidopsis thaliana. Curr. Biol. 12, 1484–1495.

Pruss, G., Ge, X., Shi, X.M., Carrington, J.C., Vance, V.B., 1997. Plant viral synergism: the potyviral genome encodes a broad-range pathogenicity enhancer that transactivates replication of heterologous viruses. Plant Cell 9, 859–868.

Qu, F., Ren, T., Morris, T.J., 2003. The coat protein of turnip crinkle virus suppresses posttranscriptional gene silencing at an early initiation step. J. Virol. 77, 511–522.

Samuel, G.H., Wiley, M.R., Badawi, A., Adelman, Z.N., Myles, K.M., 2016. Yellow fever virus capsid protein is a potent suppressor of RNA silencing that binds double-stranded RNA. Proc. Natl. Acad. Sci. USA 113, 13863–13868.

Schwartz, M., Chen, J., Janda, M., Sullivan, M., den Boon, J., Ahlquist, P., 2002. A positive-strand RNA virus replication complex parallels form and function of retrovirus capsids. Mol. Cell. 9, 505–514.

Seifers, D.L., Harvey, T.L., Martin, T.J., Jensen, S.G., 1997. Identification of the wheat curl mite as the vector of the High Plains virus of corn and wheat. Plant Dis. 81, 1161–1166.

Shi, B.J., Ding, S.W., Symons, R.H., 1997. Plasmid vector for cloning infectious cDNAs from plant RNA viruses: high infectivity of cDNA clones of tomato aspermy cucumovirus. J. Gen. Virol. 78, 1181–1185.

Silhavy, D., Molnár, A., Lucioli, A., Szittya, G., Hornyik, C., Tavazza, M., Burgyán, J., 2002. A viral protein suppresses RNA silencing and binds silencing-generated, 21- to 25-nucleotide double-stranded RNAs. EMBO J. 21, 3070–3080.

Skare, J.M., Wijkamp, I., Rezende, J.A.M., Michels, G.J., Rush, C.M., Scholthof, K.B.G.,

Scholthof, H.B., 2003. Colony establishment and maintenance of the eriophyid wheat curl mite Aceria tosichella for controlled transmission studies on a new virus-like pathogen. J. Virol. Methods 108, 133–137.

Skare, J.M., Wijkamp, I., Denham, I., Rezende, J.A.M., Kitajima, E.W., Park, J.W., Desvoyes, B., Rush, C.M., Michels, G., Scholthof, K.B.G., Scholthof, H.B., 2006. A new eriophyid mite-borne membrane-enveloped virus-like complex isolated from plants. Virology 347, 343–353.

Stewart, L.R., 2016. Sequence diversity of Wheat mosaic virus isolates. Virus Res. 231, 299–303.

Tatineni, S., French, R.C., 2014. The C-terminus of *Wheat streak mosaic virus* coat protein is involved in differential infection of wheat and maize through host-specific long-distance transport. Mol. Plant-Microbe Interact. 27, 150–162.

Tatineni, S., McMechan, J.A., Hein, G.L., French, R., 2011. Efficient and stable expression of GFP through *Wheat streak mosaic virus*-based vectors in cereal hosts using a range of cleavage sites: formation of dense fluorescent aggregates for sensitive virus tracking. Virology 410, 268–281.

Tatineni, S., Qu, F., Li, R., Morris, T.J., French, R., 2012. Triticum mosaic poacevirus enlists P1 rather than HC-Pro to suppress RNA silencing-mediated host defense. Virology 433, 104–115.

Tatineni, S., McMechan, A.J., Wosula, E.N., Wegulo, S.N., Graybosch, R.A., French, R., Hein, G.L., 2014a. An eriophyid mite-transmitted plant virus contains eight genomic RNA segments with unusual heterogeneity in the nucleocapsid protein. J. Virol. 88, 11834–11845.

Tatineni, S., Kovacs, F., French, R., 2014b. Wheat streak mosaic virus infects systemically despite extensive coat protein deletions: identification of virion assembly and cell-to-cell movement determinants. J. Virol. 88, 1366–1380.

Tatineni, S., Elowsky, C., Graybosch, R.A., 2017. Wheat streak mosaic virus coat protein deletion mutants elicit more severe symptoms than wild-type virus in multiple cereal hosts. Mol. Plant-Microbe Interact. 30, 974–983.

Vanitharani, R., Chellappan, P., Pita, J.S., Fauquet, C.M., 2004. Differential roles of AC2 and AC4 of cassava geminiviruses in mediating synergism and suppression of post-transcriptional gene silencing. J. Virol. 78, 9487–9498.

Voinnet, O., Baulcombe, D.C., 1997. Systemic signaling in gene silencing. Nature 389, 553.

Wang, M.B., Metzlaff, M., 2005. RNA silencing and antiviral defense in plants. Curr. Opin. Plant Biol. 8, 216–222.

Young, B.A., Stenger, D.C., Qu, F., Morris, T.J., Tatineni, S., French, R., 2012. Tritimovirus P1 functions as a suppressor of RNA silencing and an enhancer of disease symptoms. Virus Res. 163, 672–677.

Yu, C., Karlin, D.G., Lu, Y., Wright, K., Chen, J., MacFarlane, S., 2013. Experimental and bioinformatic evidence that raspberry leaf blotch emaravirus P4 is a movement protein of the 30K superfamily. J. Gen. Virol. 94, 2117–2128.